Electronic Supplementary Material (ESI) for Journal of Materials Chemistry C.

Supplementary Information for

Low Temperature and Rapid Formation of High Quality Metal Oxide Thin Film via Hydroxide-Assisted Energy Conservation Strategy

*Meng-Huan Jao, Chien-Chen Cheng, Chun-Fu Lu, Kai-Chi Hsiao, and Wei-Fang Su**

Department of Materials Science and Engineering, National Taiwan University, Taipei 10617, Taiwan

E-mail: suwf@ntu.edu.tw

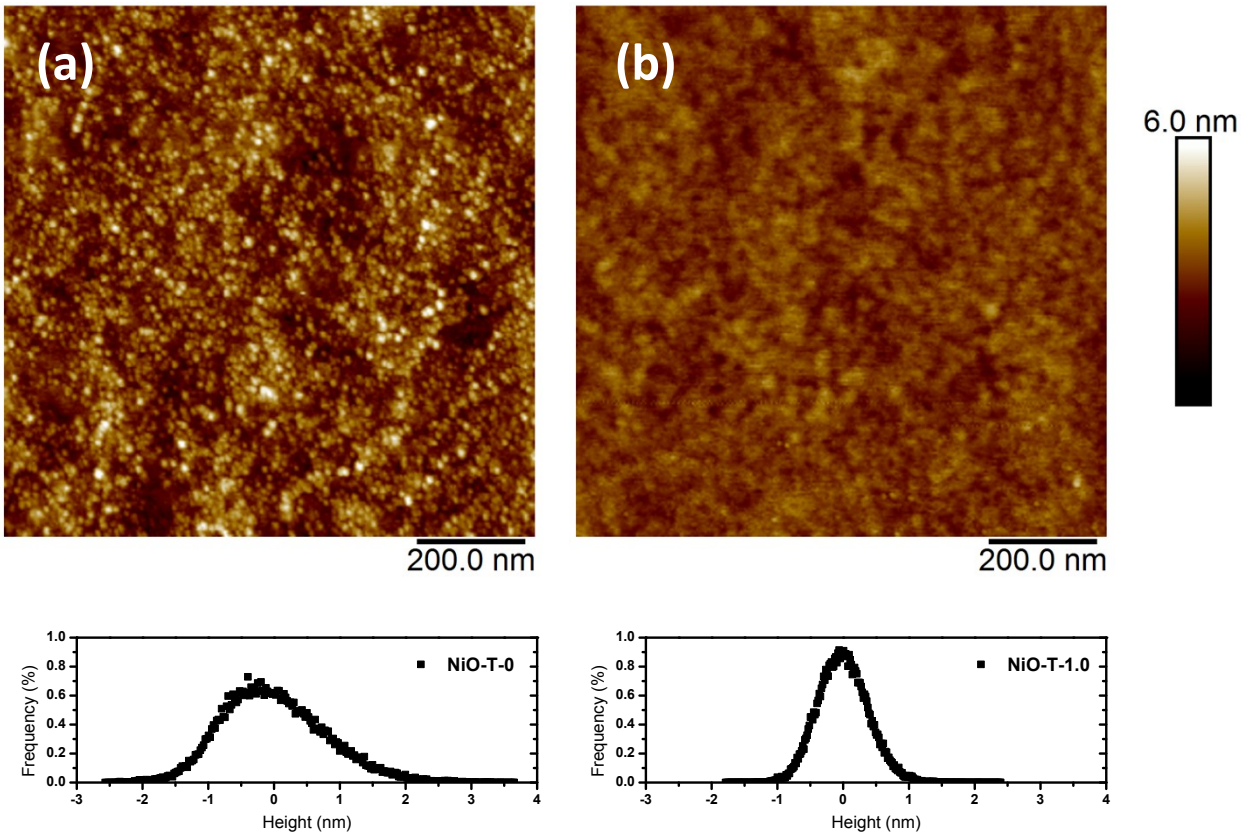

Figure S1. Atomic force microscope images of (a) NiO-T-0, and (b) NiO-T-1.0 thin films. Bottom part shows the histogram of height in each image.

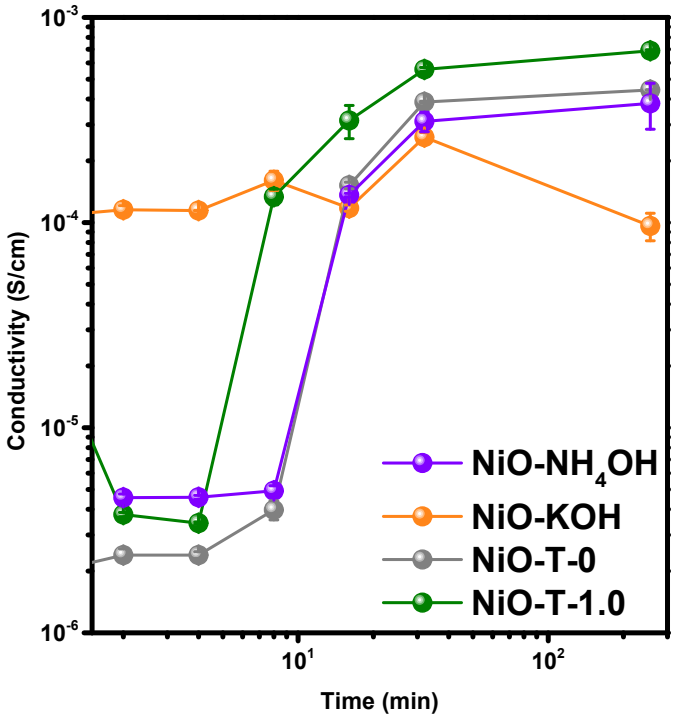

Figure S2. Conductivity evolution of nickel oxide film prepared by sol-gel process with NH_4OH or KOH. The annealing temperature was set at 250 °C.

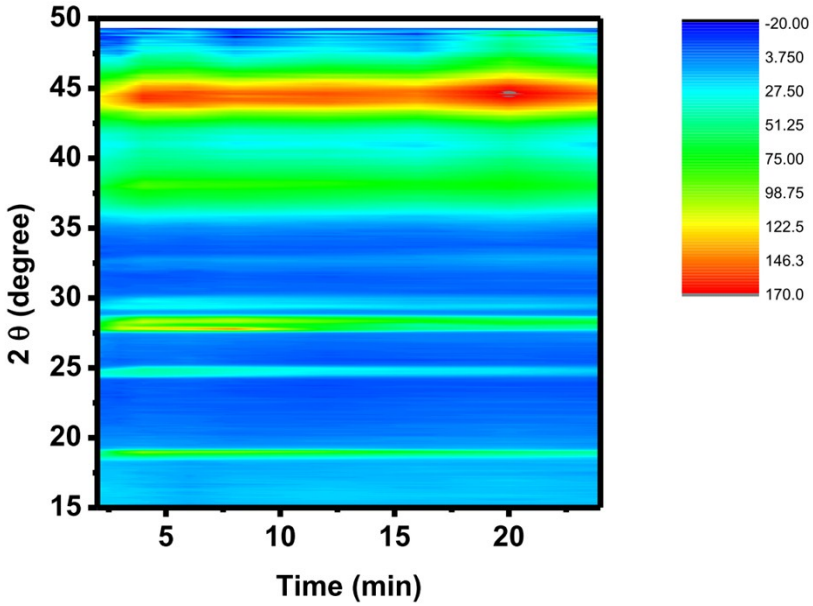

Figure S3. In-situ GIWAXS of nickel oxide thin film prepared by sol-gel process with KOH.

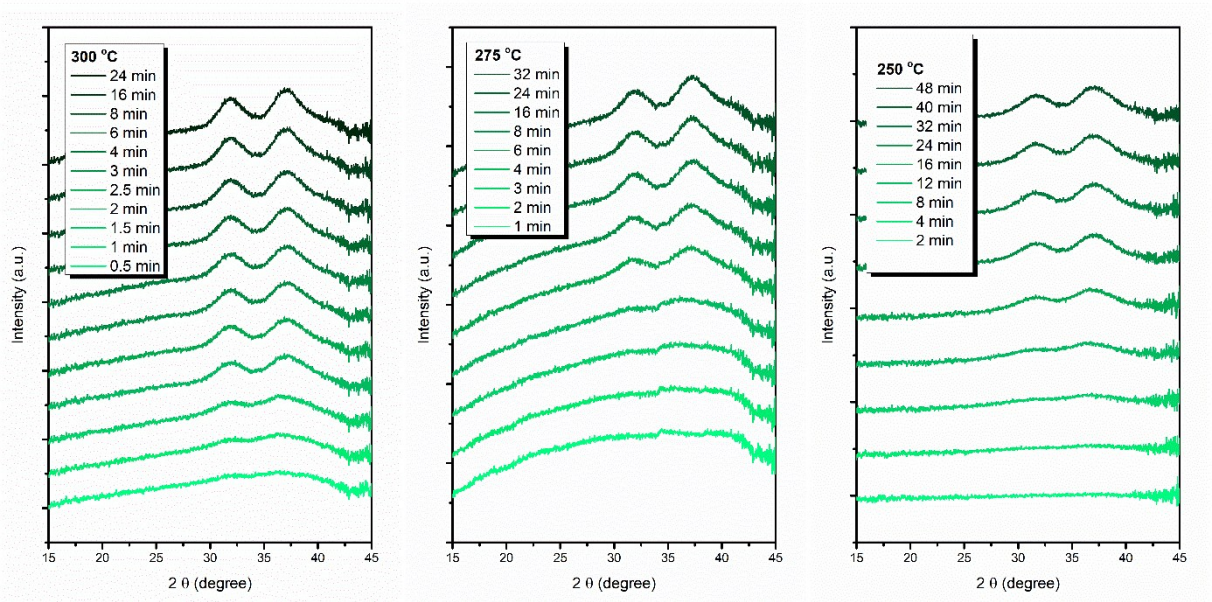

Figure S4. Time evolution of X-Ray diffraction pattern for NiO-T-0 thin film annealed at different temperature.

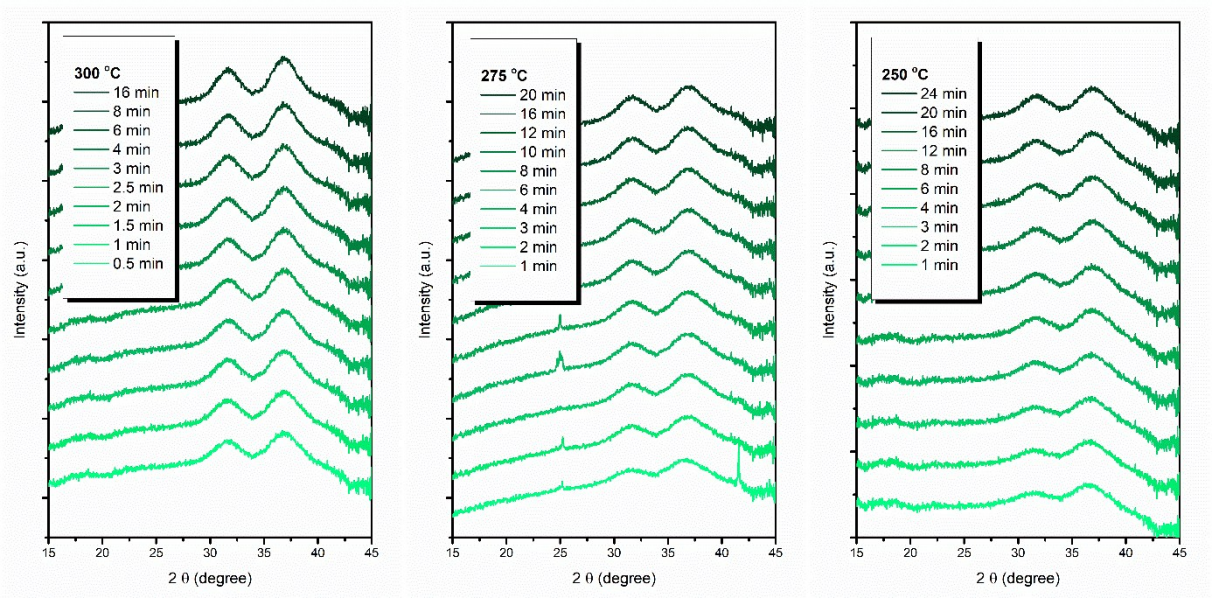

Figure S5. Time evolution of X-Ray diffraction pattern for NiO-T-1.0 thin film annealed at different temperature.

With some arrangement, we can derive the following equation from Johnson-Mehl-Avrami (JMA) equation:

$$\ln[-\ln(1-x)] = n\ln t + n\ln k$$

which we used to calculate reaction rate constant k.

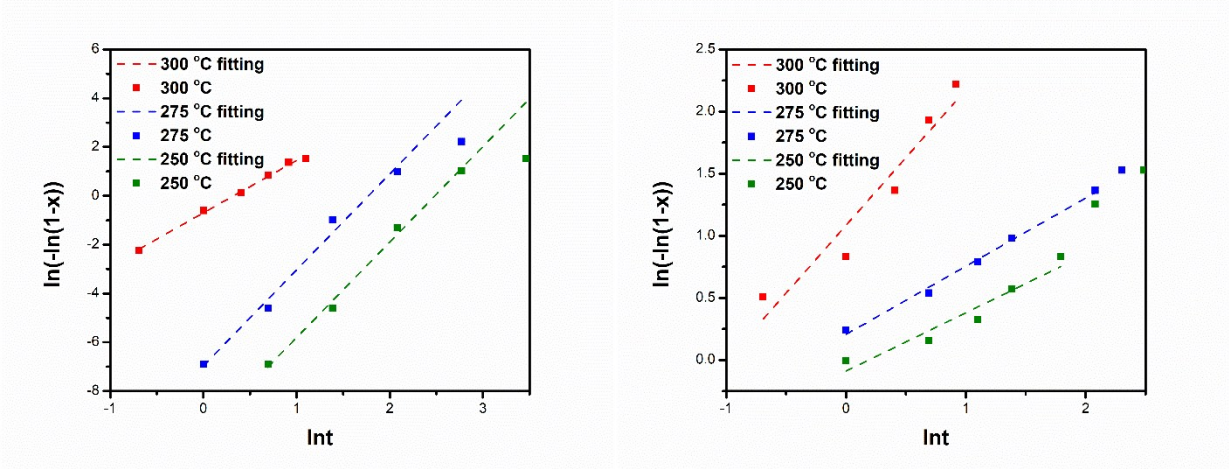

Figure S6. ln(-ln(1-x)) versus lnt plot for calculation of reaction rate constant k. The left one is data reduction from NiO-T-0, the right one is data reduction from NiO-T-1.0.

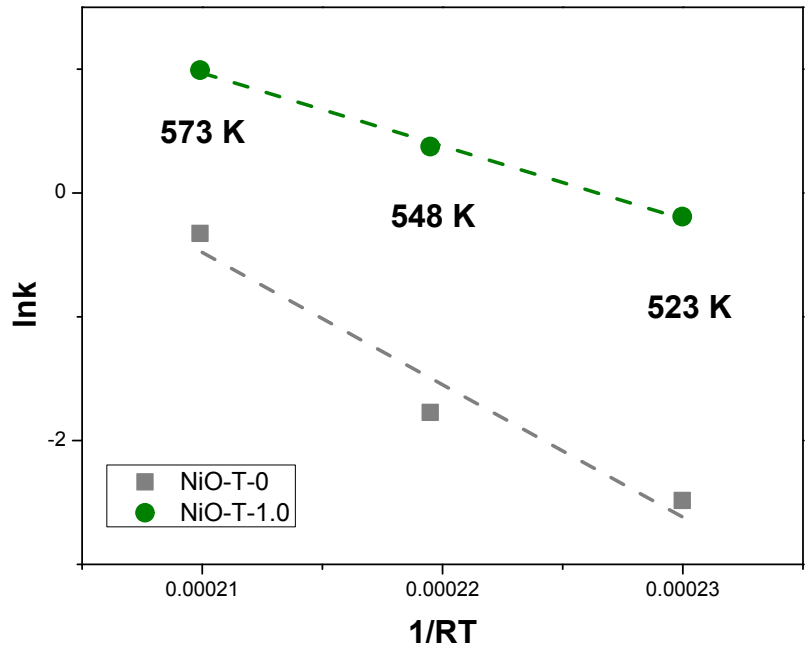

Figure S7. Plot based on Arrhenius equation to calculate activation energy. The slopes of lines were found to be -107k and -59k for NiO-T-0 and NiO-T-1.0, respectively.

Table S1. XPS peak analysis of O 1s from In_2O_3 thin films.

XPS Signal	300 °C w/o	300 °C w/	250 °C w/o	250 °C w/
Lattice O	8450	8426	6080	6521
Vacancy O	3538	3578	4777	4431
Lattice/Vacancy	2.38	2.35	1.27	1.47

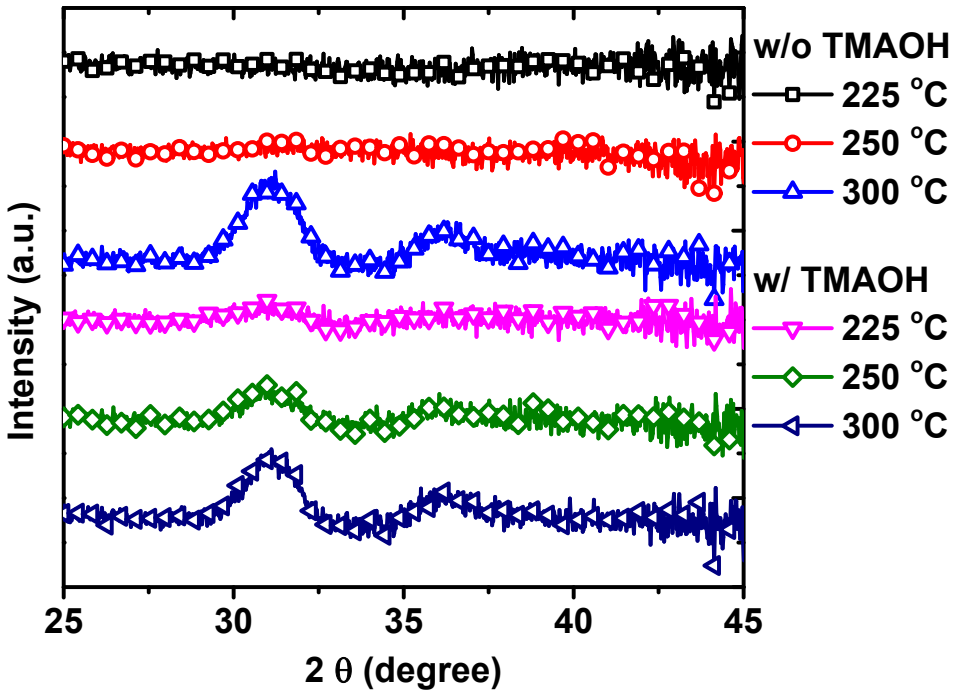

Figure S8. GIWAXS results of sol-gel In_2O_3 films by sol-gel process w/o or w/ TMAOH. The annealing temperatures were varied from 225 to 300 °C.

Table S2. Performance of OIHP photovoltaics based on NiO thin films, which were annealed at 300 °C for designed time span.

NiO w/o TMAOH				
Anneal Time (min)	V_{oc} (V)	J_{sc} (mA/cm^2)	FF (%)	PCE (%)
2	0.64 ± 0.04	0.01 ± 0.00	27.26 ± 1.32	0.00 ± 0.00
4	1.02 ± 0.00	18.25 ± 0.22	68.56 ± 3.24	12.87 ± 0.45
8	1.02 ± 0.00	17.57 ± 0.43	77.73 ± 0.85	13.99 ± 0.46
30	1.02 ± 0.00	18.86 ± 0.36	76.96 ± 1.11	14.79 ± 0.33
NiO w/ TMAOH				
Anneal Time (min)	V_{oc} (V)	J_{sc} (mA/cm^2)	FF (%)	PCE (%)
2	1.00 ± 0.01	17.58 ± 0.38	70.76 ± 2.55	12.49 ± 0.36
4	1.02 ± 0.00	18.81 ± 0.31	72.89 ± 0.88	13.99 ± 0.32
8	1.01 ± 0.00	18.67 ± 0.33	75.61 ± 1.37	14.37 ± 0.24
30	1.02 ± 0.01	19.30 ± 0.54	77.15 ± 1.13	15.24 ± 0.67

Table S3. Performance of OIHP photovoltaics based on NiO thin films, which were annealed at different temperature for 15 min.

NiO w/o TMAOH				
Anneal Temp (^{o}C)	V_{oc} (V)	J_{sc} (mA/cm^2)	FF (%)	PCE (%)
300	1.02 ± 0.00	18.36 ± 0.30	76.73 ± 0.54	14.48 ± 0.21
275	1.01 ± 0.01	18.79 ± 0.52	73.33 ± 1.60	13.98 ± 0.40
250	1.02 ± 0.00	18.69 ± 0.29	72.62 ± 1.60	13.87 ± 0.30
225	1.00 ± 0.02	0.39 ± 0.33	21.29 ± 0.57	0.08 ± 0.07
200	0.43 ± 0.05	0.00 ± 0.00	25.18 ± 2.05	0.00 ± 0.00
NiO w/ TMAOH				
Anneal Temp (^{o}C)	V_{oc} (V)	J_{sc} (mA/cm^2)	FF (%)	PCE (%)
300	1.01 ± 0.01	19.34 ± 0.28	75.11 ± 1.09	14.73 ± 0.44
275	1.01 ± 0.01	19.28 ± 0.31	75.39 ± 1.46	14.53 ± 0.43
250	1.02 ± 0.00	18.99 ± 0.41	71.03 ± 2.32	14.07 ± 0.47
225	1.02 ± 0.01	16.67 ± 0.88	71.19 ± 1.41	12.13 ± 0.59
200	1.01 ± 0.00	15.59 ± 0.59	66.25 ± 2.16	10.43 ± 0.49